Universidad del País Vasco Euskal Herriko Unibertsitatea

UNIVERSIDAD DE CANTABRIA

Master InteruniversitarioenNuevosMateriales

TRABAJO FINAL DE MASTER

SYNTHESIS AND CHARACTERIZATION OF METAL-ORGANIC FRAMEWORK AEROGELS

Presentado por: Ahmed Khalaf Reyad Raslan

Realizado en: Departamento De Química Inorgánica

Bajo la dirección del

Dr. Oscar Castillo García

Leioa, 14 de Julio 2015

Universidad del País Vasco Euskal Herriko Unibertsitatea

ZTF-FCT
Zientzia eta Teknologia Fakultatea
Facultad de Ciencia y Tecnología

Abstract:-.

Aerogels have become a material of interest to many scientists in the recent decades due to its unique physical properties which give it the potential to improve technologies in a variety of fields. MOF-based aerogel is a new branch of aerogels that has a broad range of pore sizes which encourage using them in many fields. In this project, we have synthesized and characterized several MOF-based aerogels. We have obtained chromium, vanadium, zinc, and calcium aerogels by the reaction of the metal ion and trimesic acid. The gas adsorption and electron micrography confirm the porous nature of these compounds with pores distributed from the micro- to the macropore range.

Los aerogeles se han convertido, en las últimas décadas, en un material de interés entre los científicos debido a sus propiedades físicas únicas que le dan la posibilidad de mejorar la tecnología existente en una variedad de campos. Los aerogeles basados en MOFs son una nueva rama de los aerogeles con un amplio rango de tamaño de poros que pueden permitir su utilización en diversos campos en este proyecto, hemos sintetizado y caracterizado una serie de aerogeles basados en MOFs. En concreto, hemos obtenido aerogeles con cromo, vanadio, zinc y calcio a través de la reacción del ión metálico y ácido trimésico. Las medidas de adsorción de gases y las imágenes de microscopía electrónica confirman la naturaleza porosa de estos materiales, con un amplio intervalo de tamaño de poros desde la escala micro- a la macroporosa.

Chapter1. Introduction

1.1 Definition and historical background of aerogels

Aerogels are porous materials with an open pore structure and large specific surface area. They are synthesized from a wide range of molecular precursors using the sol-gel technology and special drying methods. In 1931, Steven Kistler made the first silica-based aerogel, contained a solid matrix, which has the same size and shape of the gel. He began with a gel and extracted of the liquid, leaving a low-density solid behind. For a long time, this important material was unnoticed, due to the notorious difficulties and safety issues involved in its creation. In that time the method of, fabricating aerogels meant sending alcohol to volatile pressures and temperatures in order for it to reach its supercritical point and allow for the supercritical extraction of the gel. In the 1980's, french scientist, attempting to improve the aerogel synthesis process, he developed a process by using less-toxic materials. He switched out methyl alcohol and tetra methyl orthosilicate (TMOS) for the safer pairing of ethyl alcohol and tetraethylorthosilicate (TEOS). In the 1990's liquid carbon dioxide replaced the ethanol involved in the supercritical process. This method enables scientists to bypass the dangerous pressures and temperatures related the pure ethanol past its supercritical point. Liquid carbon dioxide has the relatively mundane requirements of 305 K and 1050 psi to be brought to its supercritical point (Fig.1).

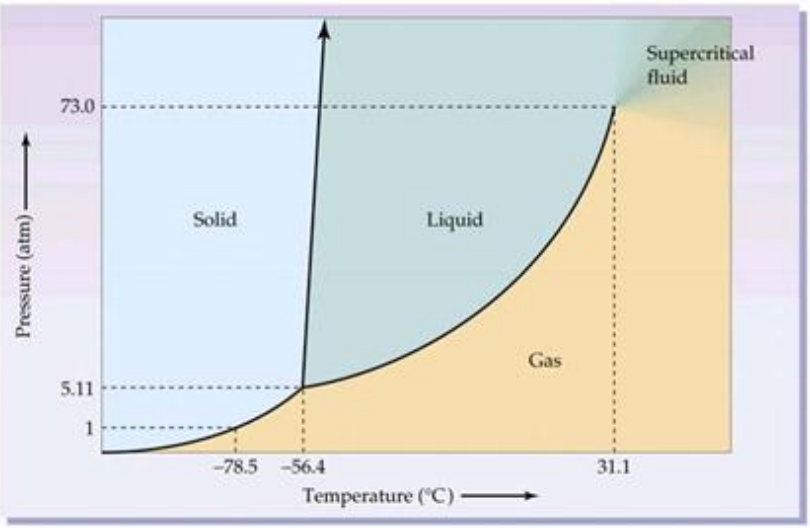

Figure 1. CO_2 phase diagram taken from reference [1].

In the 1990's, scientists found aerogel to be a new class of material, with untapped potential due to its varied and unique properties [2]. Aerogel holds the record as the solid with the lowest density and the lowest thermal conductivity; the lowest density evacuated aerogel ever produced had a density of 1.0 milligrams per cubic centimeter, so light that the sample could float in air (1.2 milligrams per cubic centimeter). SiO_2 aerogels are the most common aerogel because of, the relative simplicity, safety, and reliability of the manufacturing process. Also, many materials can be incorporated into the aerogel's structure by involving them in the gelling process, which helps to tailor the properties of the resulting sample [3].

1.2 Porous materials

Porous materials are classified depending on the characteristics of the pores they possess. In this sense, apart from the pore shape, pores can be connected among them and to the outer surface, being accessible to adsorbate molecules, or occluded (Fig. 2).

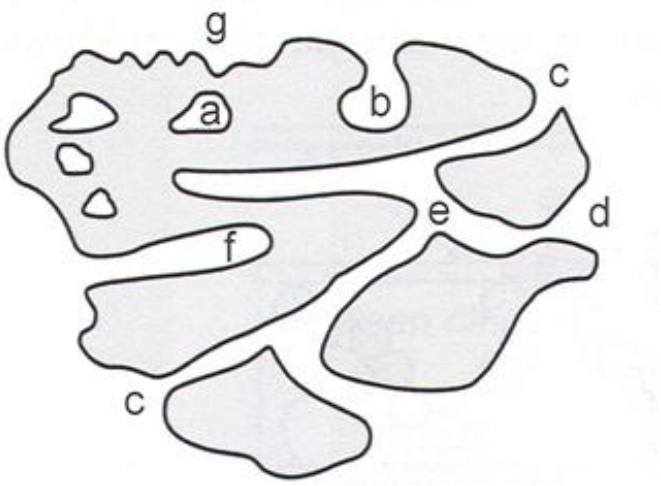

Figure 2. Different types of pores (a: closed pores; b: ink-bottle-shaped; c: cylindrical open; d: funnel; e: through pores; f: cylindrical blind; g: roughness).

Pore size is also usually employed for this purpose. There are three pore size regimes, associated with transport mechanisms:

- Microporous, smaller than 2 nm
- Mesoporous, between 2 and 50 nm
- Macroporous, larger than 50 nm.

Figure 3. Pore size classification.

1.3 Aerogels and methods for their synthesis

As previously described aerogels define a certain type of microstructure of the material, but it can be obtained from very different sources. In this sense, there is much type of aerogels:

- Silica aerogel is the most common type of aerogel, and the most extensively studied and used. It is silica-based, derived from silica gel. Silica aerogels have unusual properties such as high specific surface area (500–1200 m^2/g), high porosity (80–99.8%), low density (~0.003 g/cm^3), high thermal insulation value (0.005 W/m K), ultra-low dielectric constant (ε_r = 1.0–2.0) and low index of refraction (~1.05) (Fig. 4) [6,7,8]

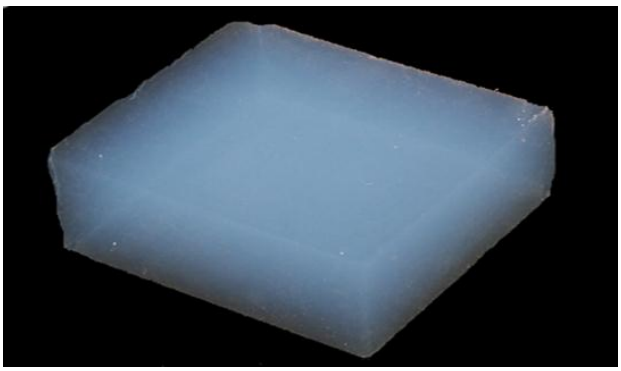

Figure 4. A piece of silica aerogel, the same type that is used in the Mars Pathfinder Rover. This is 99.8 % air.

- Carbon aerogels are composed of particles with sizes in the nanometer range covalently bonded together. They have very high porosity (over 50%, with pore diameter under 100 nm) and surface areas ranging between 400–1,000 m^2/g. [9]
- Metal oxide aerogels have unique properties they act as catalyst in various

important and advanced chemical reaction/transformation or precursors for other materials. The most common one is made with aluminium and used as catalysts, especially when "doped" with another metal, nickel–alumina aerogel is the most common combination. [10]

- MOF based aerogels represent a new generation of aerogels based related to MOFs (see following chapter) in such a way that metal centres connected through organic bridging ligands into a 3D structure but now the material has been texturized to incorporate huge void into its microstructure. The first example of this type of material corresponds to Fe-BTC aerogel (BTC being trimesate anion) (Fig. 5). [11]

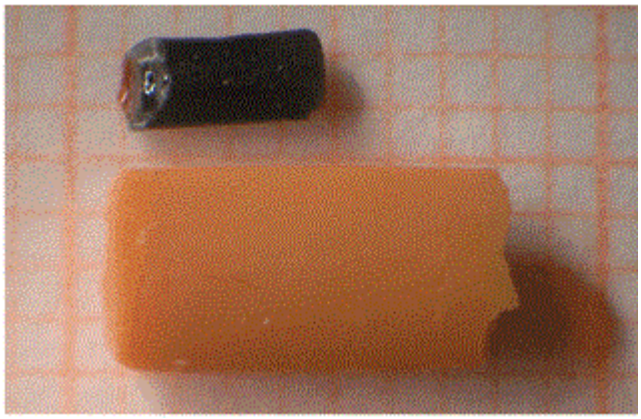

Figure 5. Photograph of an Fe-BTC aerogel obtained from 0.2 M trimesic acid solution in comparison with an air-dried xerogel of similar original size.

Almost all the above described types of aerogels are porous materials with pores that range in the meso-macro range. However, MOF based aerogel provide an even wider range of pores from the micropore regime, due to its atomic structure of the MOF, to the meso-macro range due to its microstructure. This makes them very versatile materials as adsorbent material as they are suitable for storage and carrier of small and large molecules.

1.4 Gelation mechanism

MOFs aerogels are coordination polymers with spongy network of continuous particles. To find suitable mechanism explains the gel formation some scientist suggested the formation of nanoparticle dispersions via M–O coordination as suggested by IR and their subsequent condensation into networks. In addition, those coordination polymers have been found to form spheres in solution to minimize the interfacial free energy.[12] Those nanoparticles condense together to give an open but continuous, highly porous structure. This is supported by the increase in viscosity (apparent from tilting the vials), while the formation of aerogels in the subcritical CO_2 step, happen because of the replacement of CO_2 the original solvents so the porous structure of gel may be retained to produce the aerogel.

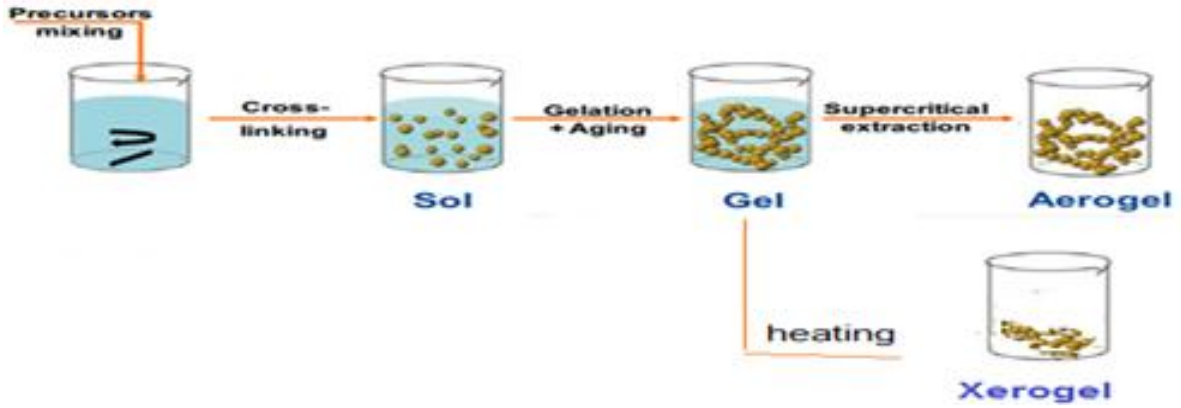

Figure 6. The synthesis procedures of the MOFs based aerogel and xerogel.

1.5 Obtaining aerogels from the gels

There are three different methods for aerogel fabrication, representing three unique solutions to the surface tension problems involved in the process. There are two fast methods such as the supercritical extraction and ambient pressure drying. Though rapid supercritical extraction is the fastest method, the ambient pressure drying method is an elegant solution, which involves chemically altering the surface of the gels to relieve tension and allow for drying at ambient pressures without a significant shrinkage of the gel. The third method, the supercritical drying process which is the one we are going to employ during this work, is a slower process but it is far more extended for the synthesis of small amounts of aerogels. This method requires either an autoclave or a critical point dryer. [13]

1.6 Metal organic Framework (MOF)

Crystalline metal-organic frameworks (MOFs) are a class of crystalline materials that consist of coordination bonds between transition-metal cations and multi-dentate organic linkers. The structure of MOFs is characterized by an open framework, usually a porous material with the pores located in the micropore regime (Fig. 7). [14]

MOFs are composed of two types of primary building units: organic ligands that act as connectors and metal centres as nodes. Using organic connectors and metal nodes with predetermined shape and geometry, it is possible to predict or design the final architecture of these materials.

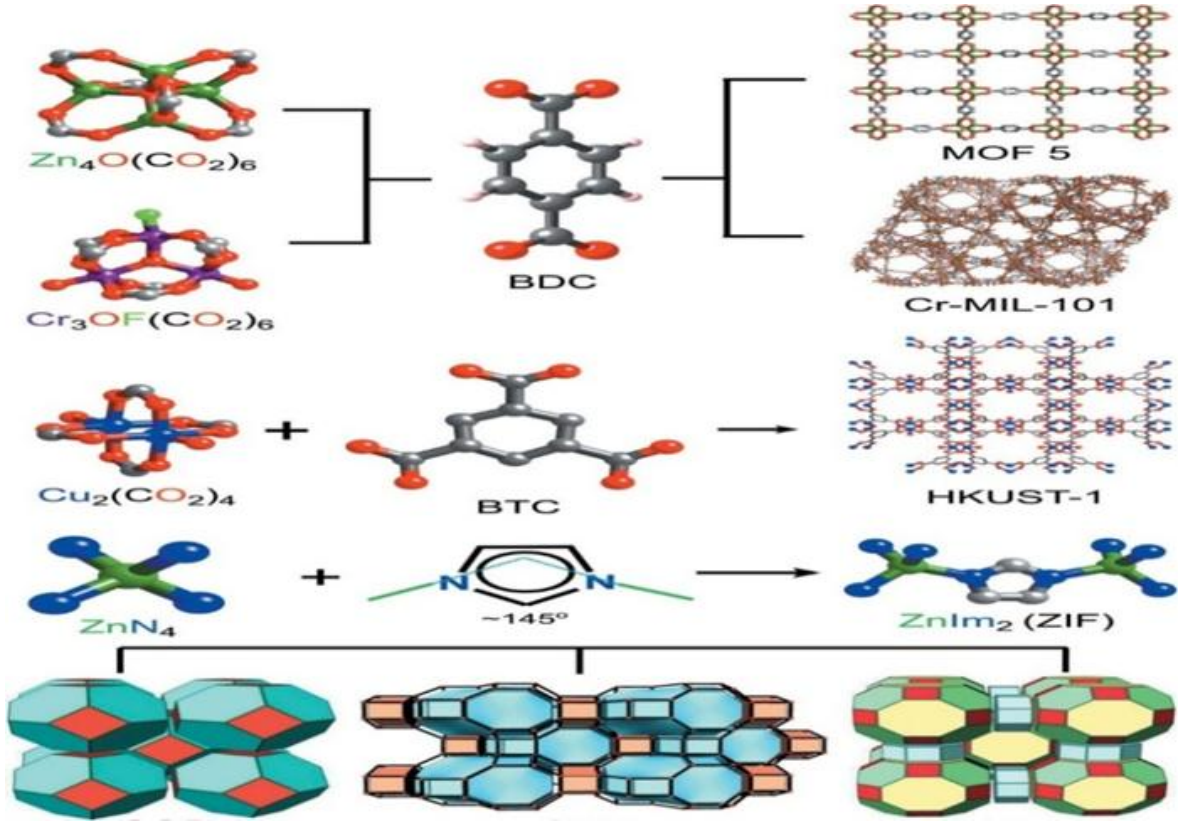

Figure 7. Examples of MOFs.

MOFs are characterized by high surface area, wide opportunities for functionalization and tunable pore structures making them appealing materials for many applications (Fig. 8). [15]

Figure 8. Different applications of MOFs.

1.7 Aims of the work

The objectives of this project is to synthesize low-density MOF-based aerogels containing broad range of pores sizes from the nanometric scale to the meso/macroscopic one and perform the characterization of their porosity. For this purpose, it is necessary to determine the synthetic conditions that allow an anisotropic particulate growth that favors the gelification process during the reaction of the metal source with the trimesic acid.

Chapter 2. Characterization techniques and synthesis

2.1 Techniques

Quantitative analysis

Elemental analyses (C, H, N) were performed on a Euro EA Elemental Analyzer, whereas the metal content was determined by inductively coupled plasma (ICP–AES) performed on a Horiba Yobin Yvon Activa spectrometer, provided by the SGIker of the University of the Basque Country (UPV/EHU).

Infrared spectroscopy

The IR spectra were recorded on a FTIR 8400S Shimadzu spectrometer of the Inorganic Department of the Science and Technology Faculty of the UPV/EHU, in the 4000–400 cm^{-1} spectral region. KBr pellets were prepared, with an approximate concentration of 2–3%. The potassium bromide was of spectroscopic quality and was previously dried at 130 ºC. The pellets were obtained at a pressure of 10 Tm.

Thermal analysis

The thermogravimetric studies (TG, DTG, and DTA) were carried out on a TA Instrument SDT 2960 thermobalance of the Inorganic Department of the Science and Technology Faculty of the UPV/EHU. The measurements were performed in an atmosphere of synthetic air (79% N_2,21%O_2) with a flow rate of 150 cm3 min–1, between 25 and 800 ºC, with a heating rate of 5 ºC min.

X–ray powder diffraction

The X–ray powder diffraction patterns were collected on a Philips X'PERT powder diffractometer of the SGIker of the UPV/EHU with Co–Kα radiation (λ = 1.5418 Å) over the range 5 < 2θ < 50º with a step size of 0.02º and an acquisition time of 2.5 S per step at 25 ºC.

Adsorption measurements

Adsorption isotherms of N_2 were measured at 77 K using a Micromeritics Tristar II 3020. Approximately 0.1 g of sample was used for analysis and placed in a glass bulb which is sealed with a rubber seal frit to prevent exposure to the atmosphere. Generally, the material is activated to remove all solvent from the pores by heating under vacuum for 4 hours at 80 ºC.

2.2.1 Cr-BTC MOF gel synthesis.

hromium(III) nitrate nonahydrate, $Cr(NO_3)_3 \cdot 9H_2O$, and trimesic acid were used as received. All solvents used were reagent grade and the H_2O used was distilled. All syntheses were performed under autoclave conditions. In a typical experiment, 1.2 g of $Cr(NO_3)_3 \cdot 9H_2O$ (3 mmol) and 0.84 g of trimesic acid (2 mmol) was dissolved in 20 ml (1:1:1) mixture of (DMF/methanol/H_2O) to give a clear dark blue solution. The resultant homogeneous solution was then left to stand at 85 ºC gelation in in a 50 ml Teflon-lined autoclaves. A gel was obtained after 30h. The result gel washed with mixture of DMF/methanol (3:2) over night, and then the gel was subjected to solvent exchange with methanol over night for three days.

2.2.2 Ca-BTC MOF gel synthesis.

Weight 0.44 g from calcium hydroxide (3 mmol) and 0.84 g of trimesic acid (2 mmol) in 20 ml of methanol, rapid shake using sonicator, a white Ca-BTC gel formed immediately then the gel was subjected to solvent exchange with methanol over night for three days.

2.2.3 V-BTC MOF gel synthesis.

0.942 g of vanadium(III) chloride and 0.84g trimesic acid were dissolved in 20 ml (1:1:1) mixture (DMF/methanol/H_2O) to give a clear dark green solution, the

resultant solution was then left to stand at 85 °C in a 50 ml Teflon-lined autoclave. A gel was obtained after 30h. The resulting gel was washed with a mixture of DMF/methanol (3:2) over night, then the gel was subjected to solvent exchange with methanol over night for three days.

2.2.4 Zn-BTC MOF gel synthesis.

Trimesic acid (0.84 g, 2 mmol), $Zn(NO_3)_2 \cdot 6H_2O$ (1.75 g, 3 mmol) were added to 20 ml DMF/H_2O = 1:1 mixed solution in a 100 mL glass beaker. The mixture was stirred at room temperature for 10 mins. The resulting solution was stirred at room temperature for a while until the solution was clear. Then 1 ml of KOH (1 M) was added and a white gel is formed. After adding 20 ml of methanol it completely dissolves. It is stirred at 100 ºC for 30 h. A white Zn-BTC gel was formed. Then the gel was subjected to solvent exchange with methanol over night for three days.

2.3 Aerogels and xerogels processing conditions

Xerogels were performed by letting the wet gels to dry at incubator for 12 h at 125 ºC. while Aerogel samples were processed in a supercritical point drier. The reactor was cooled to about 15 °C and the liquid CO_2 by the pressure difference from a CO_2 cylinder provided with the reactor. The gel is kept immersed for one hour in CO_2 at 50 bar for the exchange of methanol by CO_2. Over this time, the temperature was lowered and CO_2 replace along. While methanol removed through the waste tube. This exchange process was repeated five times. Then the temperature was raised slowly to 40 °C and the pressure was increased to 80 bars. Around 30 ºC, turbidity within the reactor due to the transition to the supercritical state was observed. Finally, the pressure was lowered very slowly while maintaining the temperature at 40°C. The employed supercritical drying machine is depicted in Figure 9.

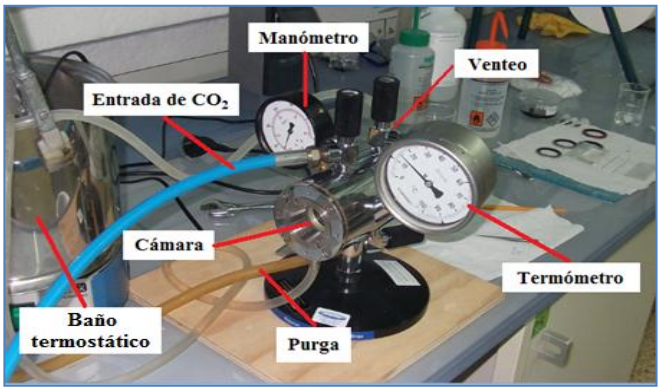

Figure 9. Supercritical drying apparatus used for the synthesis of aerogels.

Chapter 3. Results and discussion

3.1 Density of the prepared gels, xerogel and aerogels

A photo of processed samples of aero-gels, xerogels are shown in Figure 10, while (table.1) summarized density of the prepared samples.

- The prepared gel, xerogel and aerogel of Ca-BTC have white colour, they are more stable than other prepared samples, also they have a very low-density 0.11 g/cm^3 for xerogel and 0.037 g/cm^3. Ca-BTC xerogel is thermally stable even after incubating it overnight at 80 ºC, we observed that there was not any change in shape and size of xerogel after heating. There is no big difference in the volume of synthesized gel and aerogel of the Ca-BTC.
- The prepared gel, xerogel and aerogel of Cr-BTC have deep blue color; both gel and the aerogel of Cr-BTC are stable while Cr-BTC xerogel collapsed by heating, Cr-BTC has considerable law density 0.067 g/cm^3. There is a small difference in the volume of synthesized gel and aerogel of the Cr-BTC.
- The prepared gel, xerogel and aerogel of Zn-BTC have white color, Zn-BTC gel is a weak gel. There is a considerable difference in the volume of synthesized gel and aerogel of the Zn-BTC. The density of the prepared Zn-BTC aerogel is highest one it is about 0.105 g/cm^3.

- The prepared gel, xerogel and aerogel of V-BTC have deep green color, also there is a big difference in the volume of prepared gel and xerogel of V-BTC, and we cannot obtain the aerogel for V-BTC since it collapsed during CO_2 supercritical drying step. Photos of the prepared sample are shown in (fig.10).

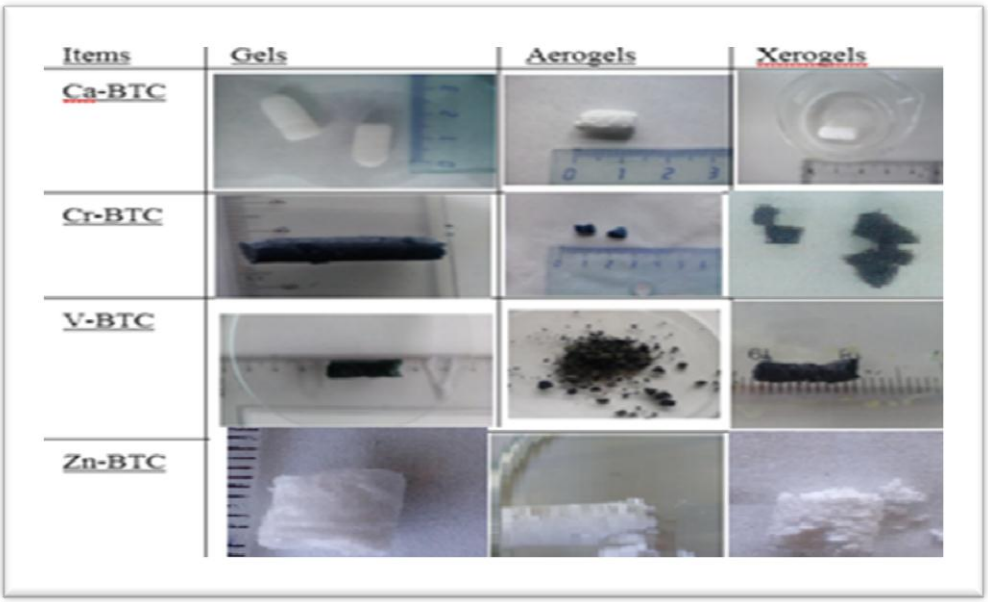

Figure 10. Samples of prepared gels, xerogels and aerogels.

Table 1. Density of the prepared aerogels, xerogels and gels.

Product	Wet gel (g/cm^3)	Xerogel (g/cm^3)	Aerogel (g/cm^3)
Cr-BTC	0.82	0.58	0.067
Ca-BTC	1.30	0.11	0.037
Zn-BTC	0.97	0.52	0.105
V-BTC	0.54	0.51	-

3.2 Elemental analysis

The data obtained using elemental analysis confirms the coordination between the trimesic acid and the metal ions. The experimental and calculated elemental analyses according to the proposed formula are gathered in table 2.

Table 2. Elemental analysis information.

Material	C (%)		H (%)		N (%)		Metal (%)		FW
	Exp.	Calc.	Exp.	Calc.	Exp.	Calc.	Exp.	Calc.	
Cr-BTC aerogel $Cr(C_6H_3O_6)_{0.78}(NO_3)_{0.65}(H_2O)_{1.80}$	29.48	29.52	3.66	2.09	3.15	3.16	18.1	18.11	1409.4
Zn-BTC aerogel $ZnK_{2.06}(OH)_{1.84}(C_9H_3O_6)_{0.71}(NO_3)_{0.08}(H_2O)_{3.268}$	19.97	19.93	2.24	2.73	0.29	0.29	16.9	16.53	389.18
Ca-BTC aerogel $Ca(C_9H_3O_6)_{0.27}\ (OH)_{1.18}(H_2O)_{0.24}$	24.39	24.44	2.8	2.07	-	-	33	33.00	120.27
V-BTC aerogel $VCl_{2.135}(C_9H_5O_6)_{0.78}(C_9H_4O_6)_{0.04}(C_3H_7NO)_{0.25}\ (H_2O)_{4.32}$	25.17	25.12	4.2	3.75	0.91	0.91	13.1	13.08	392.63

3.3 FTIR spectrum characterization

IR spectra (KBr pellet, 400 – 4000 cm^{-1}) of complex Ca-BTC,Cr-BTC, V-BTC and Zn-BTC Shows the characteristic bands of the carboxylate groups of the trimesic acid as shown in figure 11 . The absence of the characteristic bands at 1730 – 1690 cm^{-1} for protonated carboxylate groups indicates the presence of complete deprotonated form the trimesic acid for Ca-BTC , Cr-BTC and Zn-BTC aerogels, while in V-BTC show a weak absorption band at 1720 cm^{-1} which indicates presence of a free carboxylic groups. The broad band (3500 – 3200 cm^{-1}) confirms the presence of water molecules in all prepared aerogels which indicate the presence of coordinated water molecules. Also the FT-IR spectrum showed the expected absorptions for the symmetric and asymmetric vibrations of BTC (1552 and 1435 cm^{-1}), a broad band corresponding to v_{O-H} mode of water (3400 cm^{-1}), and nitrate (1385-1359 cm^{-1}) for Zn-BTC and Cr-BTC aerogels. In the case of V-BTC there are absorptions at 1730-1690cm-1 assigned to the presence of protonated BTC. We summarized the results in table 4 and figures 11 and 12.

Table 4. IR information of the aerogel samples.

- Main IR features of Cr-BTC aerogel (KBr pellet, cm^{-1}): 3422(b),3080(vw),2964(vw),2928(vw)2777(vw),2604(vw),2444(sh),2822(sh),1884(w),1764(w),1650(vs),1450(m),1380(vs),1250(w),1110(w),1060(w),1020(w),943(m),890(w),866(w),863(vw),763(s),720(s),663(s)510(s),430(m),412(vw).
- Main IR features of Ca-BTC aerogel (KBr pellet, cm^{-1}): 3400(b),2506(vw),2431(vw),23391(vw),2335(w),2324(sh),1924(vw),1884(vw),1866(vw),1862(vw),1835(vw),1795(vw),1616(s),1553(s),1433(s),1380(s),1218(m),1110(m),1057(m), 938(w), 876(s),728(s), 726(m), 526(m),456(w),433(w), 413(vw).
- Main IR features of Zn-BTC aerogel (KBr pellet, cm^{-1}): 3416(b),2616(sh),2563(vw),2483(w), 2376(w),2346(w),2156(sh),1193(w),1870(w),1633(vs),1577(vs),1438(vs),1361(s), 1110(s),1016(sh),936(sh),875(sh),840(m),760(sh),616(sh),526(m),470(sh),406(vw).
- Main IR features of V-BTC aerogel (KBr pellet, cm^{-1}): 3430(b),2650(vw),2516(vw),2333(sh),2072(w),1968(vw),1943(vw),1918(vw),1909(w),1888(vw),1865(vw),1845(w),1829(w),1812(w),1802(w),1793(w),1773(w),1720(w),1654(s),1587(vw),1451(s),1385(vs),1268(w),1276(w),1113(w),1004(w),942(w),755(m),716(m),716(m),670(vw),635(w),500(m).

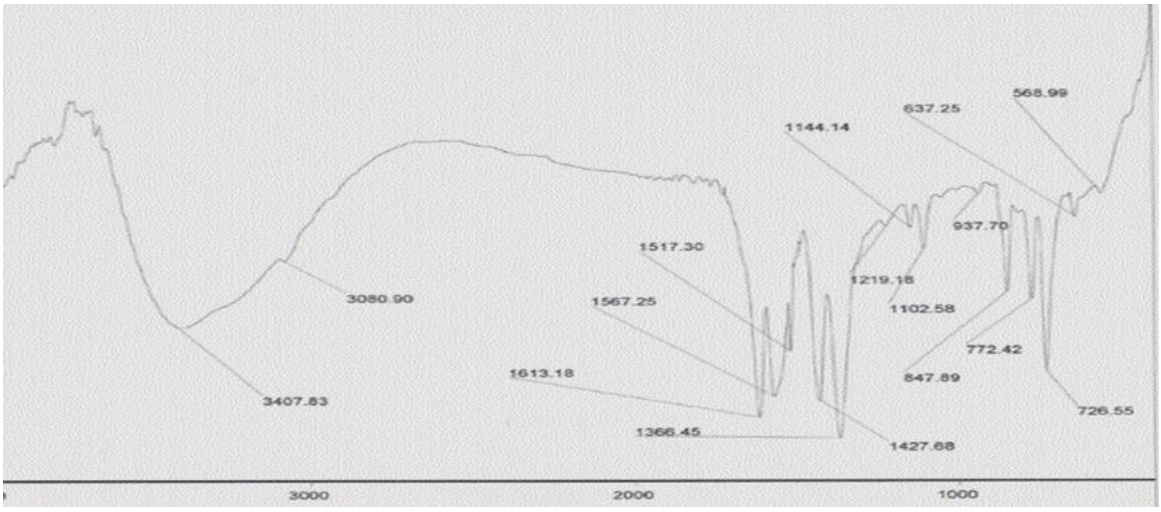

Figure 11. FT-IR absorption for trimesic acid.[18]

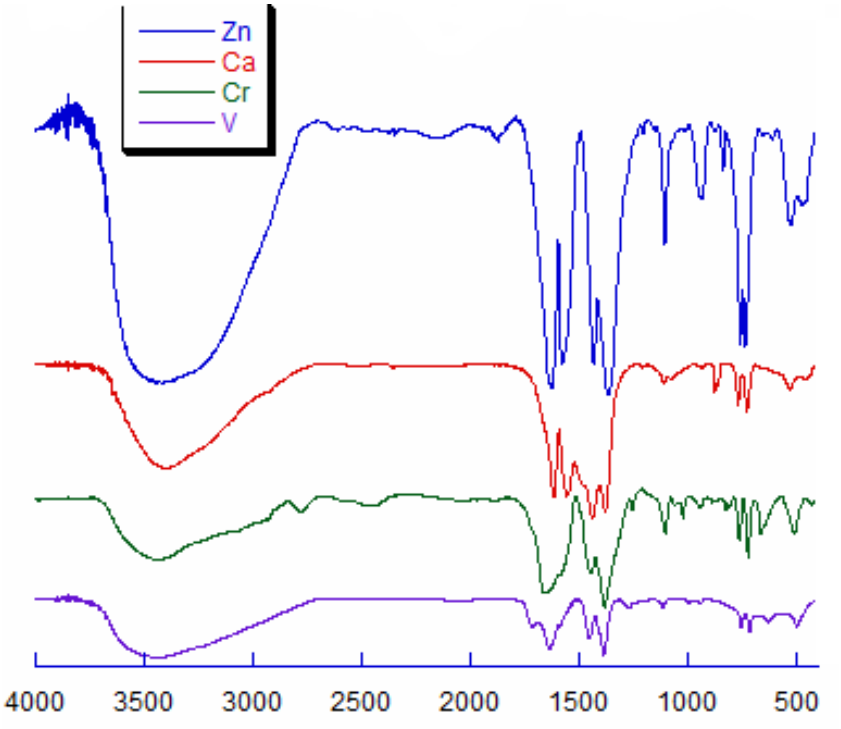

Figure 12. FT-IR absorption for the prepared aerogel of Ca-BTC, Cr -BTC, V-BTC and Zn-BTC.

3.4 thermal Analyses

The data of DTA,TGA for the prepared aerogels represents that Ca-BTC aerogel has the highest thermal stability where Ca-BTC aero gel is stable in high Temp range (up to 500°C), also we can confirm our estimated chemical formula for the prepared aerogels since the data obtained and calculated are smellier . The data is summarized in table 4. and (fig. 13).

	No of step	Ti	Tf	Δm%	∑Δm%	ΔH	Comments
Ca-BTC	1	33	138.75	11.74	11.74	endo	-solvent
	2	400	420	1.31	13.05	endo	dehydroxilation
	3	418	534	15.14	28.14	exo	not completed
V-BTC	1	47.55	98	13	13	endo	-solvent
	2	196.14	225	44.95	57.95	endo	
	3	339	421	14.63	72.58	exo	V_2O_3
Cr-BTC	1	23	83	12.14	12.14	endo	-solvent

	2	283	327	36.42	48.56	exo	Cr_2O_3
Zn-BTC	1	22	54	11.63	11.63	endo	-solvent
	2	100	143	3.9	15.53	endo	-sollvent
	3	350	388	7.82	23.35	exo	-
	4	403	418	1.53	24.88	exo	-
	5	473	524	10.97	35.85	exo	ZnO

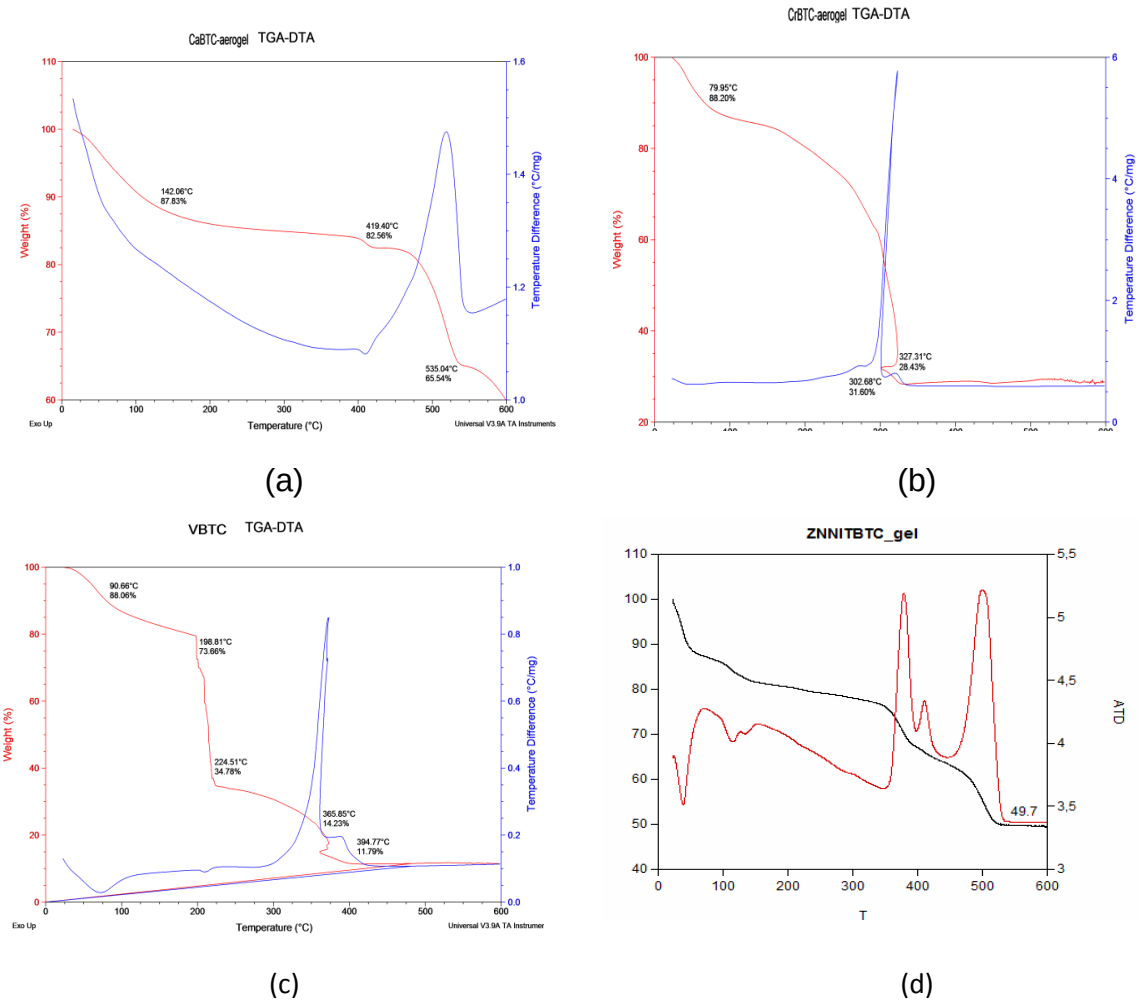

Figure 13. TG-DTA studies for prepared aerogels

3.5 X-ray powder diffraction

X-ray powder diffraction for the prepared aerogels as shown in (fig.14.a) and (fig 14.b) represent that both Cr-BTC aerogel and V-BTC aerogel are amorphous materials, while Zn-BTC aerogel and Ca-BTC show some crystallinity; Zn-BTC aerogel has three

peaks at 7.8°, 9.4° and 11.2° we found that those peak are to those of compound with reference NIWYAV (CDS database code) which has the three peaks close to those but with small shift at 8.4°, 9.9° and 10.74°. Refer to (Fig. 14.c). [16]. For Ca-BTC aerogels as shown in (fig. 14.d) has two peaks at 18.3° and 34.3° belonging to unreacted $Ca(OH)_2$. [17]

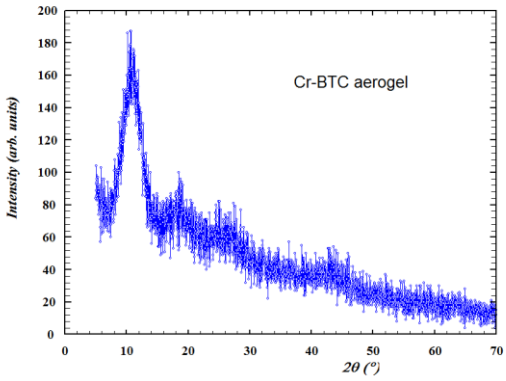

(a)

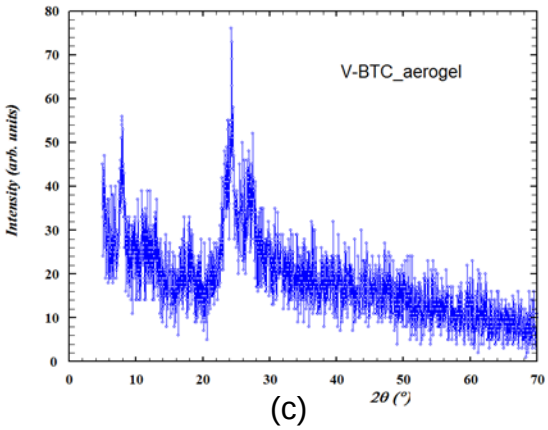

(c)

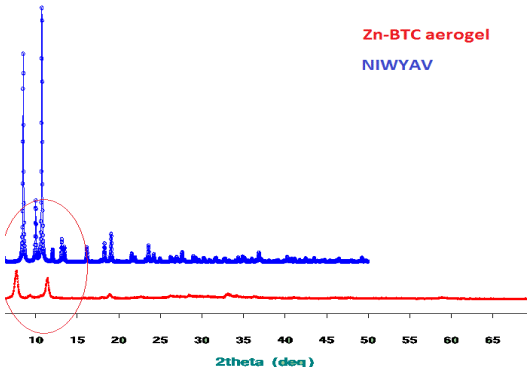

(c)

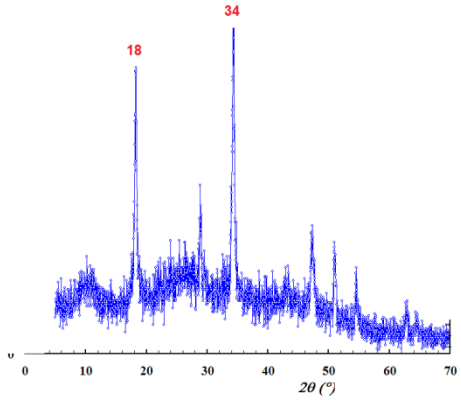

(d)

Figure 14. X-ray powder diffraction for the prepared aerogels

3.6 Scanning electron microscope (SEM)

Scanning electron microscope performed for both aerogels and xerogels, the photos of SEM have been checked by image J software to calculate the diameter and pore size.

- Ca-BTC aerogel and xerogel are fibrous macro pores material with diameter around 50-150 nm and pores size around 1 μm. We noticeds that there were some tiny crystals corresponding to the unreacted $Ca(OH)_2$. Ca-BTC xerogels has little considerable stability since it has diameter around 60 nm and pore size around 390 nm.
- Scan electron microscope for the Cr-BTC aerogel represents that Cr-BTC aerogel has particle shape with diameter less than 20 nm. It contains a wide range of pores size extended from micro to Macro pores, we estimated that those pore has pore size around 60 nm, also we can notice that Cr-BTC xerogel surface has no porosity.
- Scan electron microscope for the prepared Zn-BTC aerogel represents that Zn-BTC particle are plates with diameter about 120 nm in addition Zn-BTC aerogel has the Macro porosity nature. Zn-BTC xerogel are rode shape with very big diameter up to 1.45 μm and macro pore with size 2.1 μm.
- Scan electron microscope for the V-BTC aerogel and xerogel represents that they have no porosity.

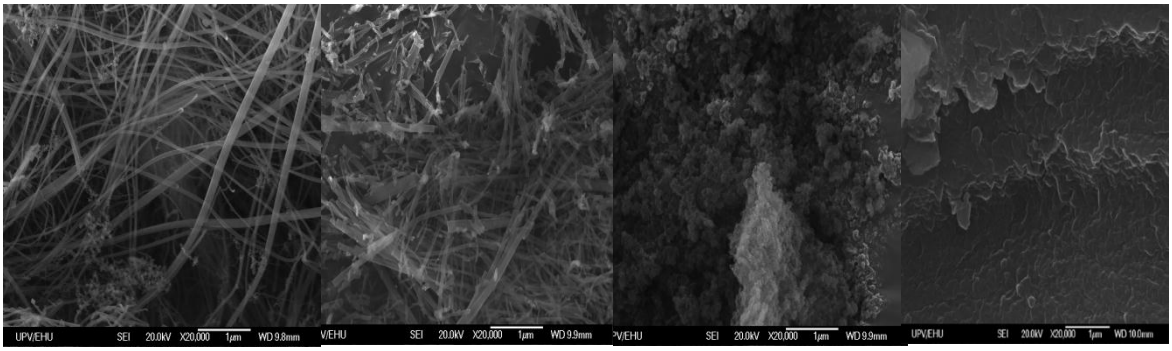

a Ca-BTC aerogel | b Ca-BTC xerogel | c Cr-BTC aerogel | d Cr-BTC xerogel

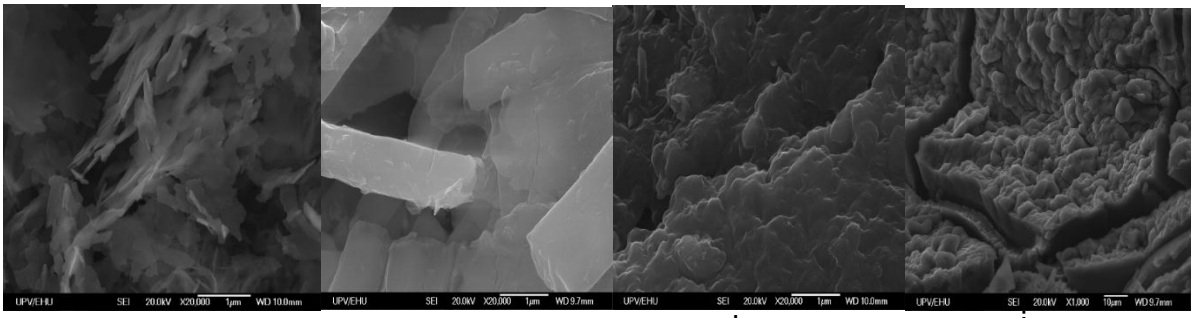

e Zn-BTC aerogel | f Zn-BTC xerogel | h V-BTC aerogel | i V-BTC xerogel

Figure 15. SEM photos for the prepared aerogels and xerogels

3.7 Nitrogen adsorption and pore analysis.

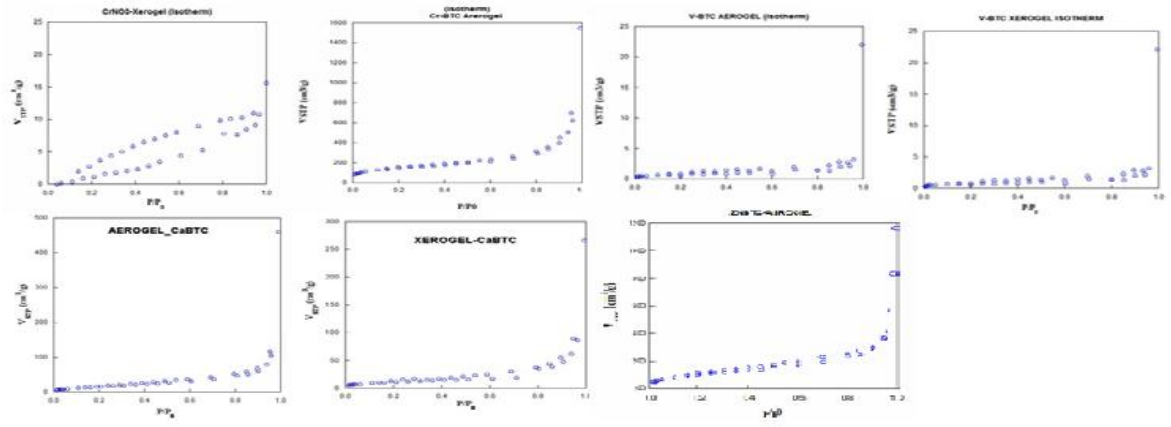

Figure 16. Nitrogen adsorption isotherms (77 K) for the prepared aerogels and xerogels of Cr-BTC, V-BTC, Ca-BTC and Zn-BTC

Calculation of specific surface area and total pore Volume by using (BET) method.

Table 3. Calculation of total surface area and pore volume.

	Areas(m2/g) ST	Smicro	Smeso/macro	Volumes (cm^3/g) VT	Vmicro	Vmacro/meso
CaBTC-aero	49,1	0,0	49,1	0,854	0,000	0,854
VBTC-aero	2,3	0,0	2,3	0,034	0,000	0,034
VBTC-xero	0,0	0,0	0,0	0,020	0,000	0,020
CrBTC-aero	524,0	190,5	333,5	2,389	0,083	2,306
CrBTC-xero	0,0	0,0	0,0	0,024	0,000	0,024
ZnBTC-aero	36,0	0,0	36,0	0,181	0,000	0,181

Table 4. Relative porosity (%) corresponding to each pore region.

	Microporosity	Macroporosity	Mesoporosity
Ca-BTC aero	0,00	28,26	71,74
Cr-BTC aero	2,42	32,06	65,52
Zn-BTC aero	0,00	30,32	69,68

Table 5. Cumulative pore volume vs pore size

Ca-BTC aerogel		Cr-BTC aero gel		Zn-BTC aero gel	
nm	cc/g	nm	cc/g	nm	cc/g
3,32233	0,0058867	3,40394	0,013735	3,05662	0,0028629
3,72465	0,0058867	3,82948	0,024853	3,41547	0,0032581
4,20718	0,011796	4,33623	0,041509	3,82872	0,0054652
4,76785	0,017938	4,94	0,059584	4,29064	0,0091949
5,95649	0,029625	6,136	0,10043	4,8821	0,0097036
8,46885	0,043098	8,78371	0,18823	6,13583	0,016603
11,9649	0,046585	12,3118	0,26406	8,84599	0,020999
17,3093	0,062737	17,82295	0,42597	11,99043	0,025602
32,16194	0,10905	32,21235	0,8718	16,38369	0,02641
230	0,33	128,88141	2,2483	29,65317	0,040229
				52,67514	0,074029
				230,56831	0,17007

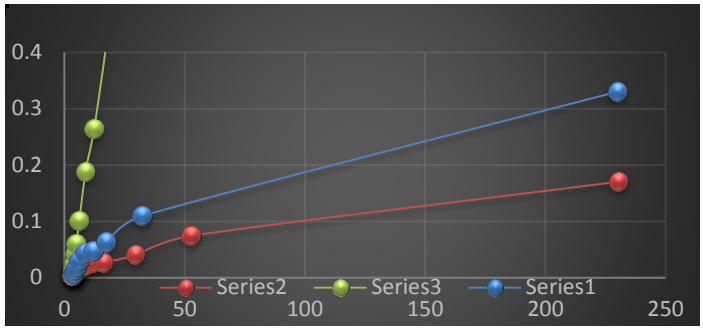

Figure 16. cumulative pore volume against pore size for the prepared aerogel of Ca-BTC aerogel, Cr-BTC aerogel and Zn-BTC aerogel.

Table (6). Pore volume corresponding to each pore region.

	Ca-BTC aerogel		Cr-BTC aerogel		Zn-BTC aerogel	
	cc/g	%	cc/g	%	cc/g	%
Vmicro	0,000	0,00	0,083	2,42	0,000	0,00
Vmeso	0,130	28,26	1,100	32,06	0,074	30,32
Vmacro	0,330	71,74	2,248	65,52	0,170	69,68
VT	0,460	100	3,431	100	0,244	100

Analyses of the surface area, pore volume, and average pore size for the prepared aerogels were performed using nitrogen adsorption isotherm at 77 K, the data analysed using The Brunauer–Emmett–Teller (BET) model to calculate the specific surface areas and the Barrett–Joyner–Halenda (BJH) model to calculate the volume and size distribution of the mesoporous.

- The macroporosity values represented in minimum value, as pore no much greater than ca.200 nm can analyse by N_2 adsorption isotherm.
- We can confirm the nature porosity of the prepared compounds and it has pores distributed from the micro- to the macro porous range.
- the porosity nature of the prepared aerogels better than those of xerogels

- Cr-BTC aerogel has the best porosity nature than other synthesized aerogel it has higher surface area, bigger pore volume, and wide pore distribution in range Micro/Macro while V-BCT has no porosity.
- Most of the aerogels showed a type IV, only V-BTC aerogel and xerogel show no adsorption properties.
- Cr-BTC aerogel has the highest surface area with 524 m^2/g because it has some Micropores which increase the total surface area , compared to Ca-BTC aerogel which is macroporous materials with total surface area around 49.1 m^2/g . While the Zn-BTC aerogel has total surface area only equal to 36 m^2/g.
- Zn-BTC aerogel has the biggest pore size more than 230,56 nm ,followed by Ca-BTC aerogel which has pore size around 230 nm, while the maximum pore size for Cr-BTC aerogel is 128,88 nm.
- Cr-BTC aerogel has the biggest total pore volume equal to 2,389 cm^3/g compered to Ca-BTC aerogel which has total pore volume around 0,854 cm3/g and Zn-BTC aerogel has 0,181 cm3/g while V-BTC aerogel and xerogel has smallest total pore volume 0,034 cm3/g and 0,020 cm3/g

4. Conclusions

We have successfully synthesized and characterized of anew three MOF -based aerogels of Ca-BTC, Cr-BTC and Zn-BTC, while V-BTC collapsed drying CO_2 super critical drying. The gas adsorption and electron micrograph confirmed the porous nature of those compounds with pores distributed from the micro- to the macropore range.Ca-BTC aerogels has wonderful properties such higher thermal stability, law density, high surface area, considerable adsorption properties ,big pores size and no toxic nature which encourage to use it in different application .

5. References

1- Daniel Sedlacek ; David Tanenbaum;(April 24, 2009): Aerogel Synthesis and Application;(09/2012);http://physastro.pomona.edu/wpcontent/uploads/2012/09/Sedlacek.pdf.

2- Bellussi, G., Carati, A., Rizzo, C. &Millini, R.: Catalysis Science &Technology, (2013), Issue 4, Page 821 -1152 .

3 Y. Cui, H. Xu, Y. Yue, Z. Guo, J. Yu, Z. Chen, J. Gao, Y. Yang, G. Qian* and B. Chen*, A luminescent mixed-lanthanide metal−organic framework thermometer, J. Am. Chem. Soc., 134(9) (2012) 3979-3982.

4 Han, S. S., Mendoza-Corte´ s, J. L. & Goddard, W. A: A Novel Self-Penetrated Framework with New Topology Basedon Rigid Ligands;Chem. Soc. Rev. (2009). 38, 1460–1476

5 Fricke, J., .J., Aerogels — highly tenuous solids with fascinating properties Non-cryst. Solids. (1988). 100, 169...

6 Fricke, J., Emmerling, Aerogels; A. J. Am. Ceram. Soc., (1992). 75, 2027

7 Fricke, J., Tillotson, T.,Thin Solid Films.(1997) 297, 212.

8 J. FrickeJ. Non-cryst. Solids, 100 (1988), p. 169

9 R.W.pekala, J.mater.sci.1989, 24, 3221.

10 Aerogel.org. Retrieved 2013-06-12, http://www.aerogel.org/?p=44

11 Rowsell,J.L.&Yaghi, O. M.Micropor.Mesopor Mater.(2004). 73, 3–14.

12 Martin R. Lohe, Marcus Rose and Stefan Kaskel*,Metal–organic framework (MOF) aerogels with high micro- and macroporosity.,w,Chem. Commun., (2009), 6056–6058

13 ChandanDey,TanayKundu,BishnuP.Biswal,ArijitMallick*,Crystallinemetal-organicframeworks (MOFs): synthesis, structure and function Structural Science, Crystal Engineering and Materials , (2014).ISSN 2052-52061.

14 Paolo Falcaro *a, Raffaele Ricco a, Cara M. Doherty a, Kang Liang: MOF positioning technology and device fabrication, Chem. Soc. Rev., (2014), 43, 5513-5560

15 Mohammad Alnaief; Irina Smirnova; Stefan Heinrich:.(2011); Process Development for Production of Aerogels with Controlled Morphology as Potential Drug Carrier Systems;(10/2011); https://tubdok.tub.tuhh.de/bitstream/11420/1011/1/phd_final.pdf

16 - Junkuo Gao,†,‡ Kaiqi Ye,§ Ling Yang,† Wei-Wei Xiong,† Ling Ye,§ Yue Wang,§ and Qichun Zhang*. Inorg. Chem. (2014), 53, 691−693.

17 Taglieri1, C. Mondelli2, V. Daniele1, E. Pusceddu3, A. Trapananti. Advances in Materials Physics and Chemistry, (2013), 3, 108-112

18 Subal Chandra Manna,a,* Soumen Mistri,a Atish Dipankar Jana b; A rare supramolecular assembly involvingion pairs of coordinationcomplexes with a host-guest relationship;Royal Society of Chemistry.(2012);http://www.rsc.org/suppdata/ce/c2/c2ce25916h/c2ce25916h.pdf